Folding of Viscous Threads in Diverging Microchannels

Thomas Cubaud and Thomas G. Mason*

Department of Chemistry and Biochemistry, Department of Physics and Astronomy, California NanoSystems Institute, University of California, Los Angeles, California 90095, USA

(Received 18 November 2005; published 20 March 2006)

We study the folding instability of a viscous thread surrounded by a less viscous miscible liquid flowing from a square to a diverging microchannel. Because of the change in the flow introduced by the diverging channel, the viscous thread minimizes viscous dissipation by oscillating to form bends rather than by simply dilating. The folding frequency and the thread diameter can be related to the volume flow rates and thus to the characteristic shear rate. Diffusive mixing at the boundary of the thread can significantly modify the folding flow morphologies. This microfluidic system enables us to control the bending of the thread and to enhance mixing between liquids having significantly different viscosities.

DOI: 10.1103/PhysRevLett.96.114501 PACS numbers: 47.20.−k, 47.15.−x, 47.60.+i, 83.50.−v

The deformations of threadlike flows in slender geometries are common and have long intrigued both scientists [1,2] and artists [3]. Viscous folding occurs in situations as familiar as pouring honey onto toast and as subtle as in the formation of large-scale geological structures [4]. Related to the buckling of slender rods and plates, viscous folding illustrates the analogy between the equations of motion for creeping flows and those describing deformations of simple elastic solids [5,6]. Although progress has been made in understanding the buckling of viscous sheets and threads as they drain onto a surface under gravity [7–10], the range of viscosities and flow rates that have been probed is limited. In addition, when a viscous thread enters another miscible liquid, the viscous resistance outside the thread considerably modifies the folding dynamics [11]. Much less is understood about this case, primarily because of the added complexity of the outer liquid.

The field of microfluidics has facilitated the study of fluid behaviors that are difficult to investigate at the macroscale [12–14]. Microfluidic devices provide precise flow geometries, greatly reduce required liquid volumes, and can be used to produce complex soft materials, such as emulsions and foams [15–17]. Microfluidic flows are usually laminar, so liquid streams remain parallel and liquids mix only by diffusion. The time scale associated with diffusion, $t_D = h^2/D$, where h is the characteristic length scale and D is the diffusion coefficient between the liquids, is typically much larger than the time scale associated with convection, $t_C = h/U$, where U is the characteristic flow velocity. Therefore, relying upon diffusion to mix liquids in simple microflow configurations is frequently impractical. As a result, innovative strategies, such as patterned surface topography [18], forced oscillatory transverse flows [19], or rotary pumps [20] have been developed to enhance mixing in microfluidics. However, numerous industrial and biological liquids exhibit widely different viscosities. Mixing liquid having large viscosity contrasts is rather complex because of the evolution of the relative mobility between the liquids as they mix in the fluidic system.

Here we study the folding of a viscous thread flowing along with a less viscous liquid into a diverging microchannel. The thread is formed by hydrodynamic focusing of a more viscous liquid flow by a less viscous liquid side flow into a square microchannel of height, $h = 100\ \mu$m [Fig. 1(a)] [21]. We use silicone oils having different viscosities ranging from 0.5 to 500 cP. The more viscous

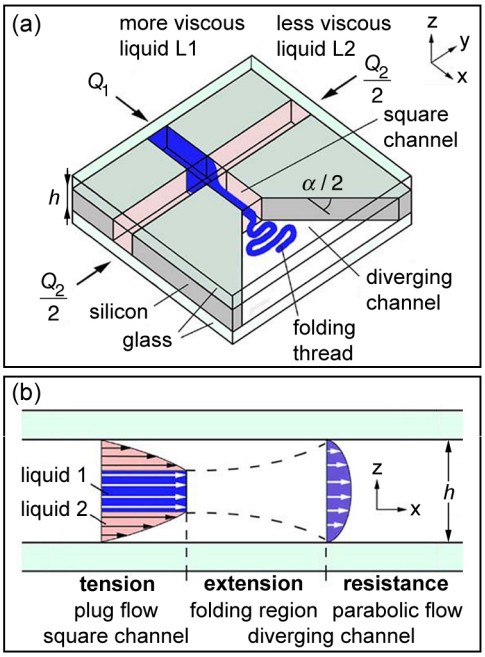

FIG. 1 (color online). Schematics of the experimental setup. (a) Diagram of a diverging microchannel module (height, $h = 100\ \mu$m). Simultaneous injection of silicone oils L1 (more viscous) and L2 (less viscous) yields a thread of L1 in the square channel. The thread enters a diverging channel characterized by the angle α. (b) Flow profiles during the folding instability (side view). Arrows indicate velocities.

liquid, L1, is injected from the central channel with a volume flow rate, Q_1, and the less viscous liquid, L2, is injected from the side channels with a total volume flow rate, Q_2. The liquids flow downstream in the square channel, before they enter the diverging channel, where the channel width increases at an angle, α. The viscous thread is essentially restricted to deform in two dimensions, which facilitates visualization and analysis, and steady-state flow patterns can be formed. Since the oils are readily miscible, surface tension is negligible; moreover, viscous forces dominate buoyancy [22], and flows are laminar [23]. The Peclet number, $\mathrm{Pe} = t_D/t_C = hU/D$, ranges between 10^3 and 10^6 since U typically ranges between 10^{-3} and 10^{-1} m/s, and D ranges between 10^{-10} and 10^{-11} m^2/s for different pairs of silicon oils [24].

In the hydrodynamic focusing geometry, Knight *et al.* [25] showed that the central liquid forms a rectangular stream of variable width when the liquids have similar viscosities $\chi = \eta_1/\eta_2 \approx 1$. For large viscosity contrasts, $\chi \gg 1$, the system minimizes viscous dissipation by adopting the configuration of a nearly cylindrical thread of the more viscous liquid in the center, lubricated by the less viscous liquid near the walls of the square channel. The thread of radius R_1 can be assumed to flow at nearly constant velocity, $U_1 = Q_1/(\pi R_1^2)$, like a solid plug, inside a sheath of the less viscous liquid, similar to the flow in a circular channel [26]. In this case, U_1 represents the maximum velocity of the surrounding liquid. Downstream, the thread and surrounding liquid enter the diverging channel creating a decelerating extensional flow [Fig. 1(a)]. Empirically, we find that the folding instability occurs for $\chi \geq 15$. Extensional viscous stresses cause the thread to bend and fold, rather than dilate, in order to minimize dissipation and conserve mass. As the thread folds, it reduces its velocity and mixes with the outer liquid. This intermediate viscosity mixture, or ''pile,'' contacts the top and bottom walls further downstream resulting in a dramatic decrease of its mobility as a function of the local viscosity [Fig. 1(b)].

Micrographs of the typical folding morphologies for various flow rate ratios, $\varphi = Q_1/Q_2$, and diverging channel angles, $\alpha = \pi/2$ and π, are shown in Fig. 2. The flow morphologies exhibit periodic oscillations depending upon the flow rates. In the diverging channel, the folds increase in amplitude, the wavelength decreases, and the thread thins. The peak folding amplitude defines an envelope between the less viscous liquid and the more viscous folded central region. As α increases, the nearly parabolic envelope becomes wider. Reducing φ decreases the thread radius, R_1, in the square channel, and folding occurs further downstream in the diverging channel. For large $\varphi \geq 0.05$, the thread begins to oscillate in the square channel, upstream from the divergence over a distance proportional to φ, typically, a few times h [Figs. 2(a)–2(d)]. For smaller $\varphi \leq 0.05$, fine filaments rapidly exit the square channel and begin folding further downstream [Figs. 2(e) and 2(f)].

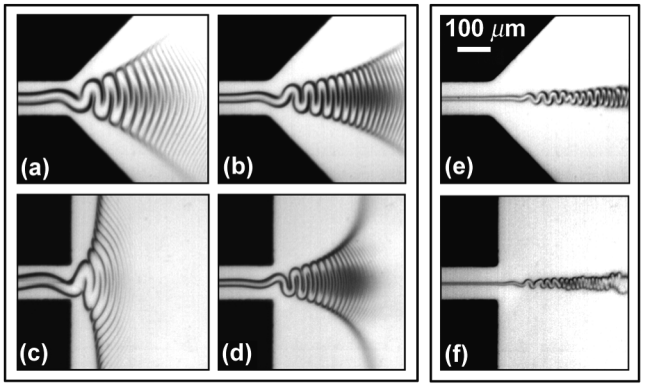

FIG. 2. Viscous folding of a thread in diverging microchannels for different channel angles α and flow rate ratios φ. The viscosities are fixed at $\eta_1 = 500$ cP and $\eta_2 = 6$ cP ($\chi = 83$). (a)–(d) The thread flow rate is fixed at $Q_1 = 5$ μl/min. (a) $\varphi = Q_1/Q_2 = 0.4$, $\alpha = \pi/2$. (b) $\varphi = 0.2$, $\alpha = \pi/2$. (c) $\varphi = 0.4$, $\alpha = \pi$. (d) $\varphi = 0.2$, $\alpha = \pi$. (e) $\varphi = 0.03$ ($Q_1 = 1$ μl/min), $\alpha = \pi/2$. (f) $\varphi = 0.02$ ($Q_1 = 1$ μl/min), $\alpha = \pi$.

Measurements of the oscillation frequency, f, as a function of the characteristic shear rate in the square channel, $\gamma = U_1/(h/2)$, for different $\chi \gg 1$, $\varphi \geq 0.05$, and α, are shown in Fig. 3. We find $f \approx \gamma/4$, independent of χ and α. To calculate γ, we measure the dimensionless diameter, $\varepsilon = 2R_1/h$, as a function of φ, upstream, away from this oscillation. Over two decades in φ, ε rises as a power law: $\varepsilon \approx \varphi^{0.6}$ [Fig. 3, inset]. This exponent is close to 1/2 corresponding to the asymptotic solution of a small cylin-

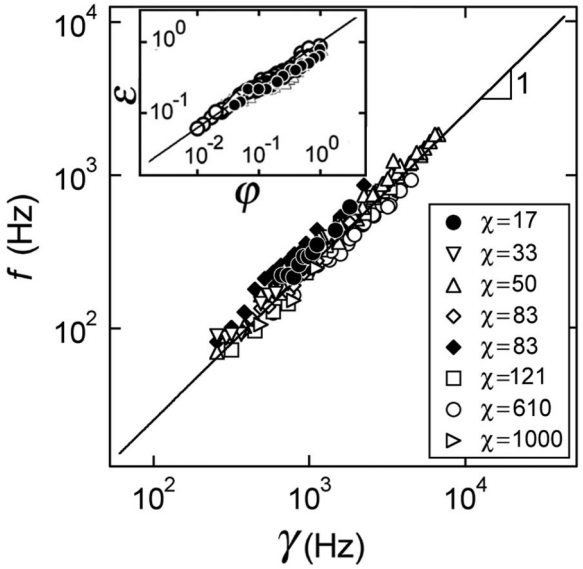

FIG. 3. Folding frequency, f, vs the characteristic shear rate, γ, for different χ and α. Line: $f = \gamma/4$. Open symbols, $\alpha = \pi/2$; filled symbols, $\alpha = \pi$. Viscosities (in cP) are: $\eta_1 = 100$, $\eta_2 = 6$ (●); $\eta_1 = 200$, $\eta_2 = 6$ (▽); $\eta_1 = 500$, $\eta_2 = 10$ (△); $\eta_1 = 500$, $\eta_2 = 6$ (◇); $\eta_1 = 500$, $\eta_2 = 6$ (◆); $\eta_1 = 100$, $\eta_2 = 0.82$ (□); $\eta_1 = 500$, $\eta_2 = 0.82$ (○); $\eta_1 = 500$, $\eta_2 = 0.5$ (▷). Inset: dimensionless thread diameter, $\varepsilon(\varphi)$; line: $\varepsilon = \varphi^{0.6}$.

drical thread ($\varepsilon \ll 1$) in a circular tube with $\chi \gg 1$:$\varepsilon = (\varphi/2)^{1/2}$. Therefore, we can estimate $\gamma \approx (8/\pi) \times (Q_1/h^3)\varepsilon^{-2} \sim Q_1^{-0.2}Q_2^{1.2}$; empirically, this implies a strong dependence of f on Q_2 and a weak dependence on Q_1:$f \approx 2/(\pi h^3)Q_1^{-0.2}Q_2^{1.2}$. The folding frequency in this regime, $\varphi \geq 0.05$, depends only on the rate of injection of the liquids and the square channel size, h, analogous to the viscous regime of a liquid rope coiling on a surface [10].

Since intermolecular diffusion can considerably modify the local viscosities, the morphology of the pile also depends on the absolute values of the flow rates and the viscosities. To investigate the crossover between diffusive and convective folding regimes, we use a highly diffusive oil for the surrounding liquid, $\eta_2 = 0.5$ cP. Because of the small molecular sizes, molecules of less viscous oils diffuse faster than molecules of more viscous oils [24]. By varying Q_1 and φ, we obtain a diffusive-to-convective folding micrograph diagram [Fig. 4]. For very low flow rates ($Q_1 \leq 1$ μl/min), the two oils have time to interdiffuse in the square channel; this leads to a small viscosity gradient between the liquids and inhibits significant folding. Considerable intermolecular diffusion occurs for low flow rates, $Q_1 \leq 5$ μl/min [Figs. 4(a)–4(c)], and is negligible for larger flow rates, $Q_1 \geq 20$ μl/min [Figs. 4(d)–4(f)]. In the diverging channel, the sinuous shape of the thread increases the interfacial area between the liquids and the less viscous liquid is trapped between the folds that thin in the extensional shear. This mechanism enhances mixing between the liquids. For small flow velocities, striations of the more viscous oil are convected away from the bends of the thread into the less viscous liquid beyond the primary envelope. Near the diverging walls, the outer liquid remains essentially pure [Figs. 4(a)–4(c)]. The rate of mixing is different inside and outside the primary envelope. In the pile, the lower viscosity liquid must diffuse into the stretched threads. For moderate flow velocities, mixing becomes significant inside the pile and the folding mechanism reduces the effective viscosity in the center of the pile. This allows the central region of the pile to flow faster than its boundaries, producing curved viscous ripples having a distinct central bulge along the direction of the flow [Figs. 4(f) and 4(e)]. For larger velocities, the thread boundary remains sharp; thus, there is a locally high viscosity gradient between the two liquids. The interplay between folding and the high viscosity gradient leads to the formation of heterogeneous viscous mixtures downstream [Fig. 4(f)]. In this case, the heterogeneous deposition of the thread creates a pile having nonperiodic viscous ripples. As opposed to purely diffusive flows [14], viscous folding offers the practical ability to rapidly enhance mixing between liquids having different viscosities in microfluidic devices.

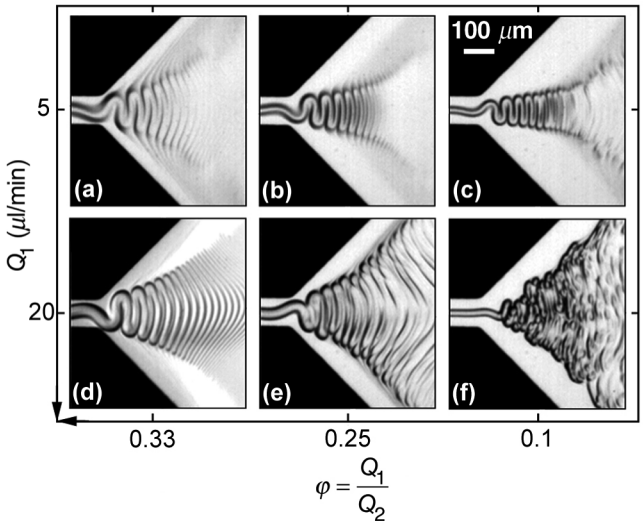

FIG. 4. Diffusive-to-convective folding micrograph diagram: Q_1 vs φ. Thread viscosity: $\eta_1 = 500$ cP, outer viscosity: $\eta_2 = 0.5$ cP ($\chi = 1000$). (a)–(c) Folding with strong diffusive mixing ($Q_1 = 5$ μl/min). (d)–(f) Folding with weak diffusive mixing ($Q_1 = 20$ μl/min). Heterogeneous viscous mixtures are formed at low φ and high Q_1.

The flow of the pile can become unsteady for large χ and large Q_1. The self-adjusting downstream boundary conditions in combination with the folding lead to more complex transient flow morphologies, which we call "subfolding" [Fig. 5]. Subfolding is characterized by the periodic alternation of two folds upward followed by two folds downward. The folds remain within an envelope that is still parabolic overall. Subfolding patterns appear to have distinct branches further downstream. Although the folding frequency, f, is largely insensitive to the flow of the pile, the appearance of subfolding indicates that a self-consistent solution to the thread trajectory can include more complex periodic solutions than a simple oscillation. The symmetry breaking in the deposition of the folds, induced by the convecting boundary conditions, may be interpreted as a transition from periodic to chaotic (i.e., heterogeneous) folding.

Our study shows that a rich variety of viscous folding morphologies can be generated in microfluidic devices. We

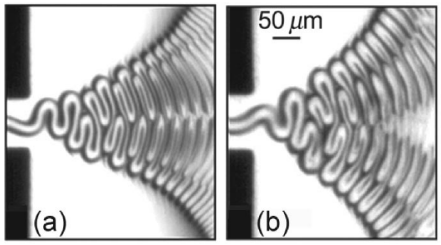

FIG. 5. Subfolding of a viscous thread. The folding thread oscillates alternatively between the upper and lower sides of the folding envelope, creating subfolds within folds ($\eta_1 = 200$ cP, $\eta_2 = 0.5$ cP, $\chi = 400$). These folds are stretched in the extensional shear flow, producing structures resembling branches downstream. Flow rates (μl/min): (a) two apparent branches: $Q_1 = 12$, $Q_2 = 50$. (b) Four apparent branches: $Q_1 = 20$, $Q_2 = 100$.

obtain many unanticipated and potentially useful flow phenomena: oscillatory folding, folding modified by strong diffusion, heterogeneous folding, and subfolding. We show that folding induced by diverging channels considerably enhances passive mixing between liquids having different viscosities. In particular, this type of geometry could be used to inject and mix a controllable amount of less viscous liquid into a more viscous liquid. This study opens up new directions for controlling liquid interfaces [27] and exploiting viscous instabilities in systems dominated by viscous forces, such as microfluidic flows. In particular, viscous folding is promising for the study of dynamic interactions between a wide range of complex and reactive fluids. Solving the hydrodynamic equations of motion for the shape and trajectory of the boundary-free threads inside the channel is a theoretical challenge that would provide key insights into the rich nature of viscous folding. Simulations that include the full treatment of the convection-diffusion equations for the folding and stretching thread could lead to a microchannel design that optimizes the mixing.

We thank Professor Chih-Ming Ho and the CMISE for the use of the high-speed camera. We also thank Dr. John McTague for supporting this work. We are grateful to Professors Robijn Bruinsma and Alex Levine for suggestions and discussions.

*Author to whom correspondence should be addressed.
Email address: mason@chem.ucla.edu.

[1] A. Bejan, in *Annual Review of Numerical Fluid Mechanics and Heat Transfer*, edited by T. C. Chawla (Hemisphere, Washington, DC, 1987), Vol. 1, p. 262.
[2] L. Mahadevan, W. S. Ryu, and A. D. T. Samuel, Nature (London) **392**, 140 (1998).
[3] A. Goldsworthy and J. L. Thompson, *Wall* (Harry N. Abrams, New York, 2000).
[4] A. M. Johnson and R. C. Fletcher, *Folding of Viscous Layers* (Columbia University Press, New York, 1994).
[5] J. Teichman and L. Mahadevan, J. Fluid Mech. **478**, 71 (2003).
[6] A. Boudaoud and S. Chaieb, Phys. Rev. E **64**, 050601(R) (2001).
[7] J. O. Cruickshank and B. R. Munson, J. Fluid Mech. **113**, 221 (1981).
[8] M. Skorobogatiy and L. Mahadevan, Europhys. Lett. **52**, 532 (2000).
[9] N. M. Ribe, Phys. Rev. E **68**, 036305 (2003).
[10] M. Maleki *et al.*, Phys. Rev. Lett. **93**, 214502 (2004).
[11] R. W. Griffiths and J. S. Turner, Geophysical Journal **95**, 397 (1988).
[12] C. M. Ho and Y. C. Tai, Annu. Rev. Fluid Mech. **30**, 579 (1998).
[13] H. A. Stone, A. D. Stroock, and A. Ajdari, Annu. Rev. Fluid Mech. **36**, 381 (2004).
[14] T. M. Squires and S. R. Quake, Rev. Mod. Phys. **77**, 977 (2005).
[15] A. S. Utada *et al.*, Science **308**, 537 (2005).
[16] T. Cubaud *et al.*, Phys. Rev. E **72**, 037302 (2005).
[17] K. Meleson, S. Graves, and T. G. Mason, Soft Mater. **2**, 109 (2004).
[18] A. D. Stroock *et al.*, Science **295**, 647 (2002).
[19] F. Bottausci *et al.*, Phil. Trans. R. Soc. A **362**, 1001 (2004).
[20] H.-P. Chou, M. A. Unger, and S. R. Quake, Biomed. Microdevices **3**, 323 (2001).
[21] Double-side polished silicon wafers (100 μm thick) are etched through in the section where the liquids make contact, the square channel and the diverging channel using deep reactive ion etching. Borosilicate glass pieces are anodic bonded to the top and bottom of the silicon chips. A high-intensity fiber optic light is positioned below the module and a high-speed camera is mounted on a microscope above the module to image sharp variations of refractive index n, ranging from 1.375 to 1.453, at the interface of the liquids. Liquids are injected in the devices using syringe pumps.
[22] Given the microchannel thickness h and the volume flow rates of injection ($1 < Q < 200$ μl/min), buoyancy forces are negligible compared to viscous forces: $(g\Delta\rho h^4)/(\eta Q) < 10^{-2}$, where g is the acceleration due to gravity and $\Delta\rho$ is the density difference between the oils.
[23] The maximal Reynolds number for our liquids and flow conditions, $\mathrm{Re}_{\mathrm{max}} \approx \rho_2 Q_2/(\eta h^2) \approx 50$, with the minimal viscosity $\eta_2 = 0.5$ cP, having the density $\rho_2 = 0.764$ g/cm^3, and with the maximal flow rate $Q_2 = 200$ μl/min. Although Re can be larger than unity, all flows are laminar.
[24] N. Rashidnia *et al.*, Int. J. Thermophys. **22**, 547 (2001).
[25] J. B. Knight *et al.*, Phys. Rev. Lett. **80**, 3863 (1998).
[26] Q. Cao *et al.*, Canadian Journal of Chemical Engineering **81**, 913 (2003).
[27] J. Atencia and D. J. Beebe, Nature (London) **437**, 648 (2005).